**Supplementary data to article:**

**Involvement of the metabolic sensor GPR81 in cardiovascular control**

**Supplementary Figure S1**

Correspondence and translation of potency rank across the assays used for selection of GPR81 agonists from the primary in vitro screen to acute in vivo testing. Graphs plot potency estimates obtained in different assay pairs for individual GPR81 agonists. (**A**) Correlation between potency values obtained for inhibition of forskolin induced lipolysis in primary rat adipocytes and inhibition of forskolin stimulated cyclic adenosine monophosphate (cAMP) in Chinese hamster ovary (CHO) cells transfected with rat GPR81 (the primary screen applied in the High through-put screen (HTS)). (**B**) Potency to inhibit forskolin stimulated lipolysis in primary human adipocytes versus primary rat adipocytes. (**C**) Potency to suppress fasting plasma free fatty acid (FFA) in rats *in vivo* versus potency to inhibit forskolin stimulated lipolysis in primary rat adipocytes in vitro. In all figures AZ1 and AZ2 are represented by red and purple triangles, respectively.

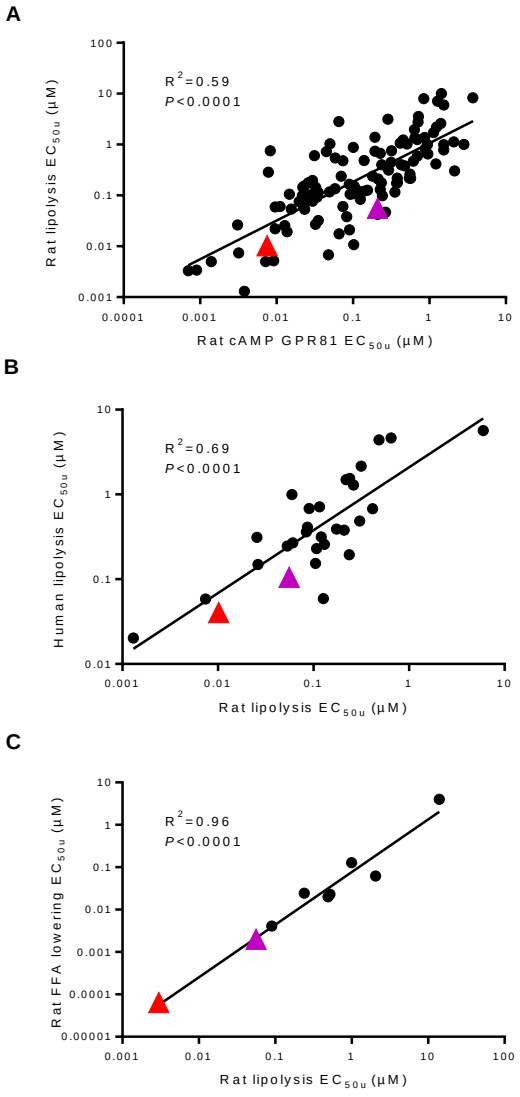

**Supplementary Figure S2**

GPR81 deficiency has no major impact on baseline diurnal blood pressure profile. Adult wild type (WT, black symbols) or GPR81 deficient (KO, grey symbols) mice were implanted with carotid catheter/radio-telemetry devices and allowed ≥2 weeks to fully recover their pre-operative body weights. Mean arterial pressure (MAP) and heart rate (HR) were then monitored around the clock in conscious unrestrained animals. Dark period between 18:00 and 06:00. The average profile for 2 consecutive (baseline) days was obtained in each animal immediately prior to the AZ2/vehicle, 4 day treatment period (responses plotted in Figure 6). (**A**) MAP profile. No significant difference in either 24 h averaged MAP or the 24 h MAP time profile (analysed by repeated measures ANOVA) between GPR81 KO and WT mice. (**B**) HR profile. No significant difference in 24 h averaged HR but a tendency for shape of the profile to differ between KO and WT mice (repeated measures ANOVA, Genotype × Time interaction *P*=0.024) although there were no significant differences in HR at any particular time period (Bonferroni corrected, P>0.05). Results show mean±SEM, n=5-6.

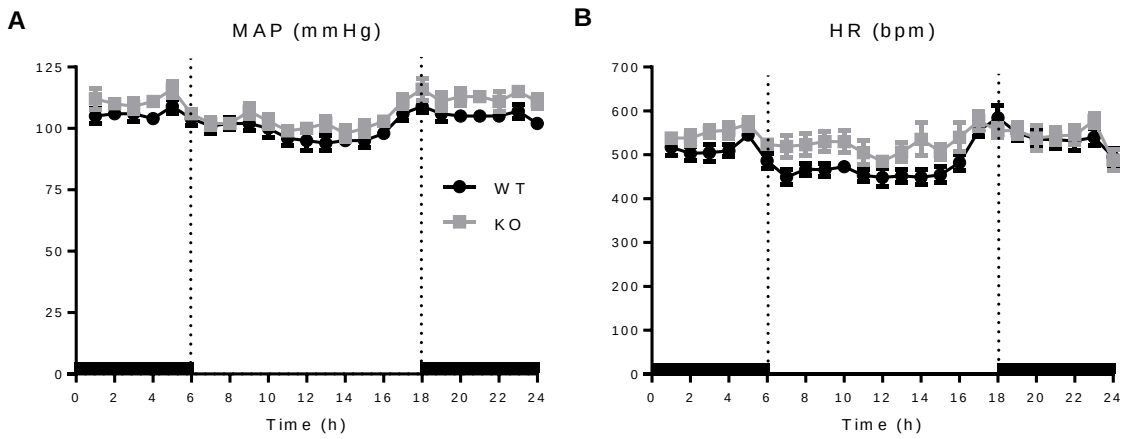

**Supplementary Figure S3**

Cardiovascular effects of the GPR81 agonist, AZ2, in anesthetized, ventilated dogs. Supporting information to Figures 8 and 9. (**A**) Experimental protocol. Following a 15 min baseline period, AZ2 was administered i.v. in five consecutive escalating doses (as specified in the figure), each given over a 15 min period and ending at 90 min. Each dose was given at the same fixed volume infusion rate. A washout period of 30 min followed the dosing period. Responses to AZ2 (red) or vehicle (blue) treated dogs are expressed relative to the mean values during the baseline period. (**B**) Central venous pressure. (**C**) Descending coronary artery flow. (**D**) Coronary resistance. Results are Mean±SEM. (**B**) (**C**) *P* is Treatment × Time interaction (repeated measures ANOVA). **P*<0.05, ***P*<0.01, ****P*<0.001 AZ2 versus control at the corresponding time period, n=4.

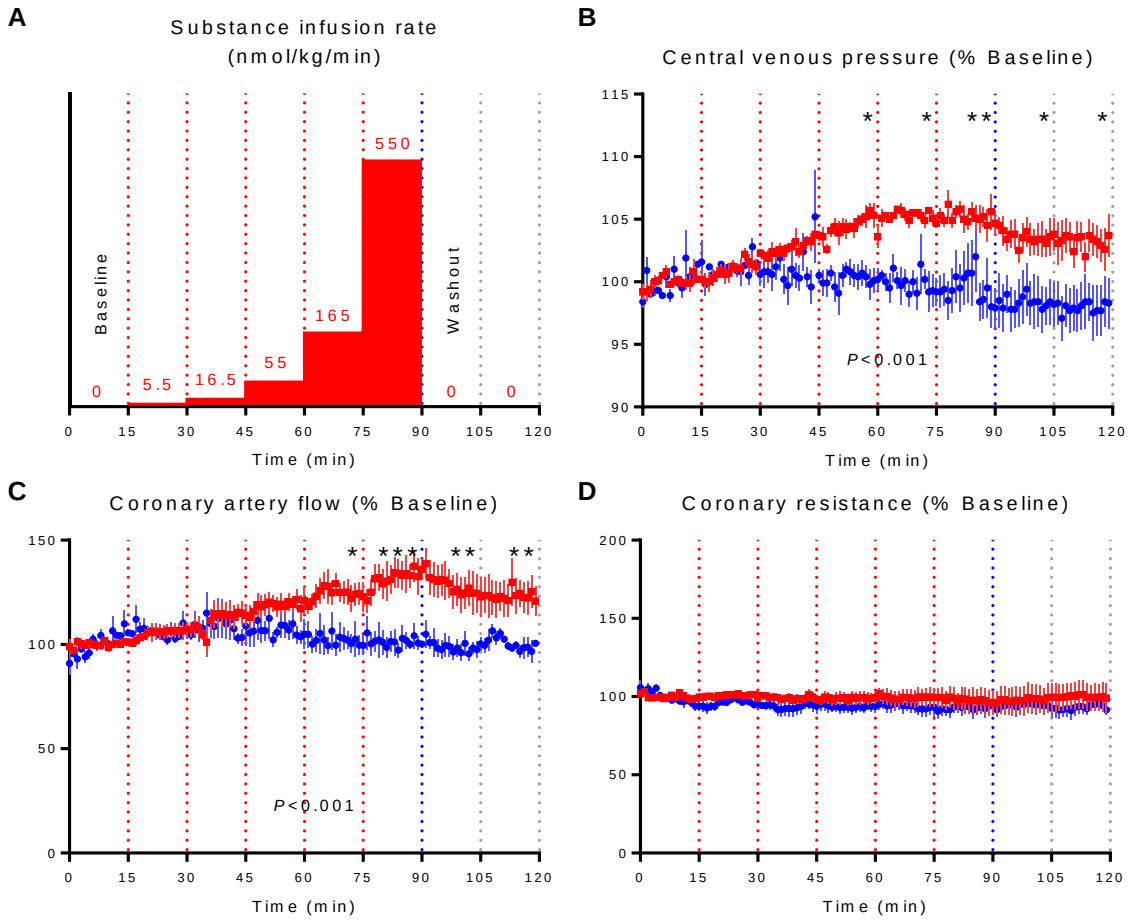

**Supplementary Figure S4**

Pilot experiment showing that α-adrenoceptor (αAR) blockade lowers mean arterial pressure (MAP) and disrupts renal blood flow (RBF) autoregulation leading to a severe reduction in RBF. An adult male Wistar rat was anesthetized and implanted with jugular and carotid catheters. Laparotomy was then performed and a flow probe attached to the left renal artery, abdomen closed and the animal was left for a 1h recovery. MAP, shown in black with scale on the left-hand vertical axis and RBF, shown in grey with scale on the right-hand axis, were monitored continuously. α-AR blockade was achieved using phentolamine (15mg/kg, i.v.), given at t=0 min.

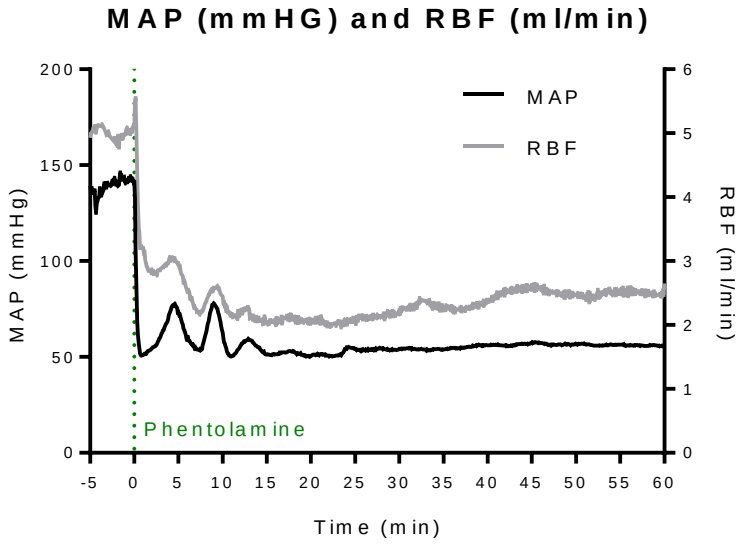

**Supplementary Figure S5**

Possible signalling mechanisms linking GPR81 agonism to vasoconstriction in specific tissues including kidney. Three vascular cell types participate: endothelial cells (EC); sympathetic nerves (SN); and vascular smooth muscle cells (VSM). GPR81 receptors are postulated to reside on vascular endothelial cells of specific tissues of the body, notably kidney, but not heart or skeletal muscle. The situation with a pharmacological GPR81 agonist (or hyperlactatemia) is shown on the right of the dotted line. Sufficient agonist engagement of GPR81 stimulates the abluminal release of endothelin-1 (ET-1) from secretory granules (SG) from EC, perhaps via a Gi-mediated reduction in cAMP levels. Exocytosis of Weibel-Palade bodies (WPB) is not stimulated. Liberated ET-1 activates ET receptor A (ETR) on adjacent VSM to induce contraction. In addition, ET-1 activates local ETR on the pre-synaptic terminals of SN. This could increase synaptic norepinephrine (NE) concentrations in the synapse by suppressing the re-uptake of NE, through inhibition of NE transporter (NET) and/or by stimulating the release of NE. In the synapse, increased NE activates α1-adrenoceptors (αAR) to stimulate VSM contraction. The resting, baseline situation with low levels of the endogenous GPR81 agonist (lactate) is depicted to the left of the dotted line. In this state, GPR81 agonism is insufficient to stimulate ET-1 release and therefore lacks the downstream consequences.

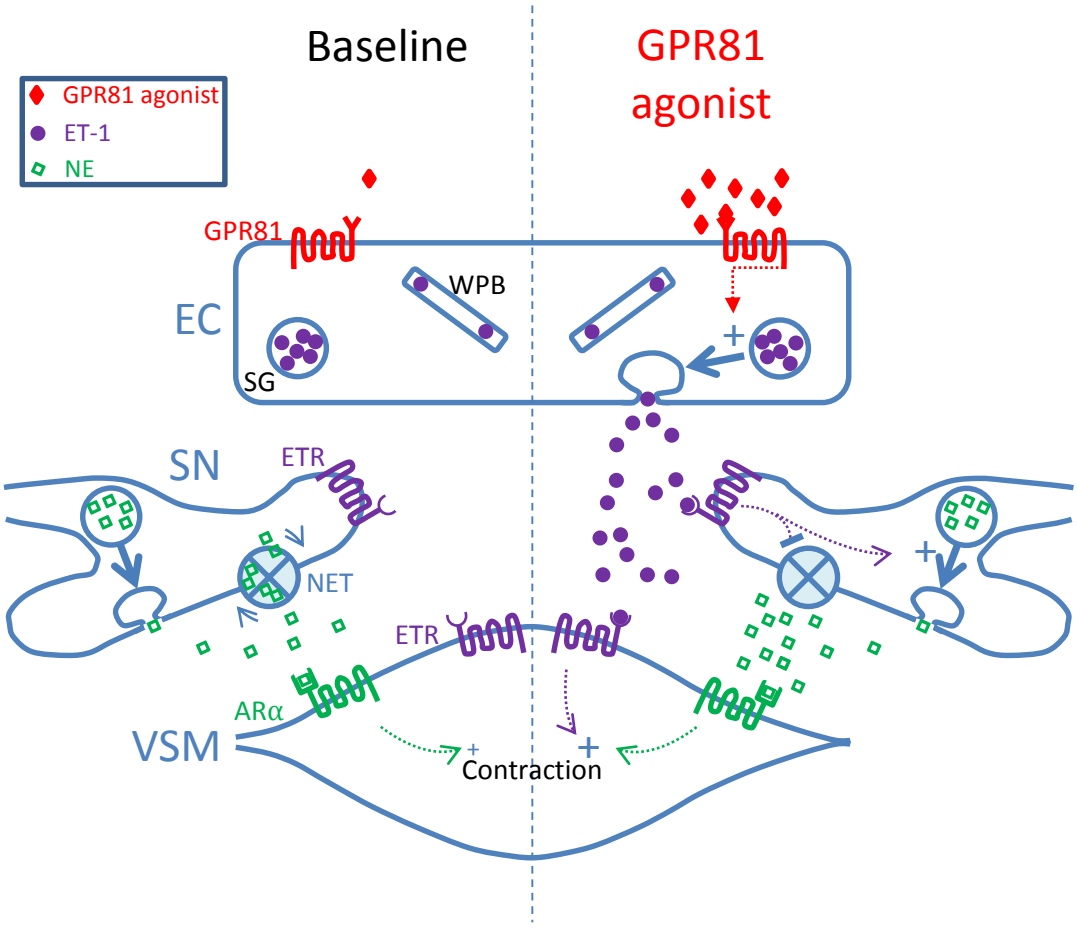

**Supplementary Figure S6**

GPR81 gene targeting strategy. Schematic diagram of the targeting vector used to generate Gpr81 null mice. Closed triangles indicate *loxP* sites open triangles indicate *frt* sites.

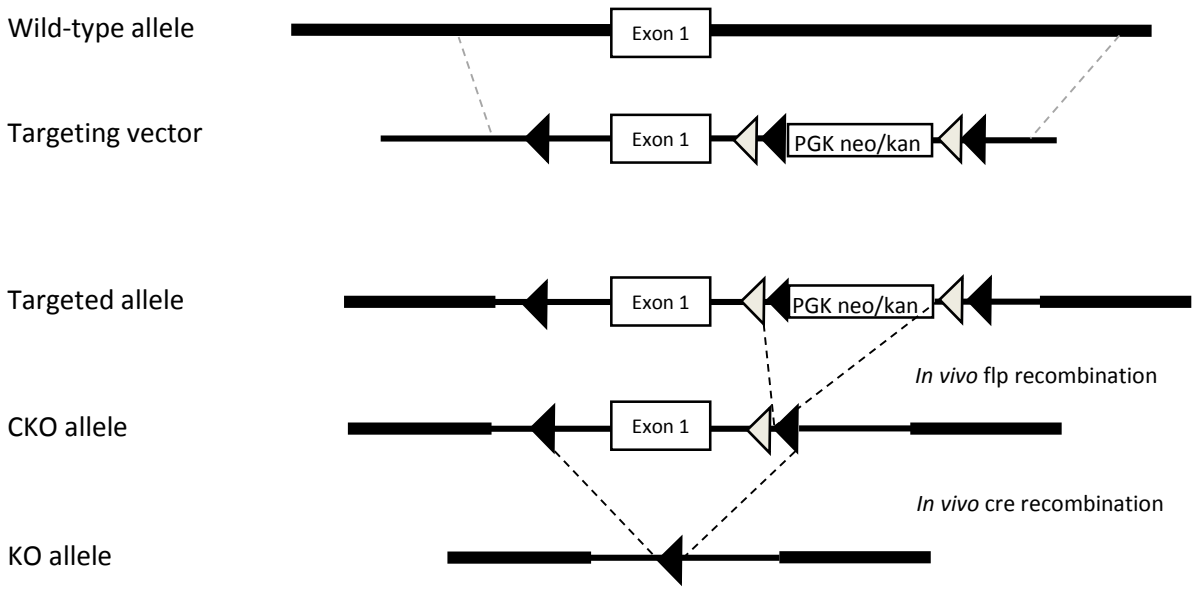

**Supplementary Tables**

**Table S1**

Effects on body weight, plasma biomarkers and exposure in diet induced obese mice (DIO) following 27 days of treatment with vehicle or AZ1 (20 µmol/kg). Male mice, fed a high-fat (60% calories) diet for 15 weeks, were daily dosed for 3 weeks by oral gavage, with either vehicle or AZ1 (20 µmol/kg), at the beginning of the dark cycle. Body weights, initial and final at day 0 and 27 of treatment, respectively. Blood sample collected 4 h after final dosing and after 4 h fasting. HOMA-IR, an index of insulin resistance, is the product of plasma glucose and insulin concentrations. FFA, free fatty acid.

| | **Vehicle** | **AZ1** |
|---|---|---|
| Initial body weight (g) | 47.5 ± 0.9 | 47.3 ± 0.8 |
| Final body weight (g) | 46.9 ± 0.07 | 44.8 ± 1.0 |
| Body weight gain (g) | -0.6 ± 0.3 | -2.6 ± 0.5** |
| Plasma Glucose (mM) | 14.2 ± 0.7 | 14.4 ± 0.8 |
| Plasma Insulin (nM) | 1.0 ± 0.1 | 0.3 ± 0.1*** |
| HOMA-IR (mM*nM) | 13.3 ± 1.7 | 4.3 ± 0.9** |
| Plasma Fructosamine (µM) | 30.5 ± 2 | 32.3 ± 1.8 |
| Plasma FFA (mM) | 0.55 ± 0.04 | 0.41 ± 0.04* |
| AZ1 (µM) | | 2.5 ± 0.18 |

n=8/group. Comparisons between vehicle and AZ1 treatment were made using Students t-test. *$P$<0.05, **$P$<0.01, ***$P$<0.001

**Table S2**

Two weeks of treatment with the GPR81 agonist, AZ1 (p.o. 20 µmol/kg/day), improves glucose control and insulin sensitivity in ob/ob mice without influencing body weight gain. Body weights, initial and final at day 0 and 14 of treatment, respectively. Blood sample collected 3 h after final dosing and after 3 h fasting. HOMA-IR, an index of insulin resistance, is the product of plasma glucose and insulin concentrations. FFA, free fatty acid.

| | **Vehicle** | **AZ1** |
|---|---|---|
| Initial body weight (g) | 35.2 ± 1 | 35.4 ± 0.9 |
| Final body weight (g) | 40.5 ± 1.1 | 40.9 ± 0.8 |
| Body weight gain (g) | 5.4 ± 0.1 | 5.5 ± 0.3 |
| Plasma Glucose (mM) | 20.5 ± 2.2 | 15.8 ± 1.4 |
| Plasma Insulin (nM) | 5.07 ± 0.5 | 2.1 ± 0.2*** |
| HOMA-IR (mM*nM) | 99.5 ± 8.9 | 32.7 ± 3.9*** |
| Plasma Fructosamine (µM) | 43 ± 6.4 | 27 ± 2.7[A]* |
| Plasma FFA (mM) | 0.59 ± 0.06 | 0.47 ± 0.03 |
| Plasma AZ1 (µM) | LLOQ | 3.1 ± 0.3 |

[A]two values were below the detection limit 17 µM and were set to this level. n=8/group. LLOQ, below lower limit of quantification. Comparisons between vehicle and AZ1 treatment were made using Students t-test. *$P$<0.05, ***$P$<0.001.

**Table S3**

Absolute values of baseline cardiovascular variables in a study to investigate the potential roles of the endothelin (ET) and adrenergic systems in the AZ2 induced pressor effect. Supporting information to Figure 7. Adult male Wistar rats were anesthetized and implanted with jugular and carotid catheters, then left to stabilize for 2 h. Mean arterial pressure (MAP), heart rate (HR) and an index of total peripheral resistance (TPRi = MAP/HR) were averaged over the 10 min baseline period immediately prior to Vehicle/AZ2 administration. The dual ET-A/B receptor antagonist, bosentan (15 mg/kg), or the $\alpha$-adrenoceptor antagonist, phentolamine (10 mg/kg), were given i.v. prior to the baseline period.

| | MAP (mmHg) | HR (bpm) | TPRi (mmHg.min) |
|---|---|---|---|
| Vehicle | $122 \pm 5$ | $367 \pm 10$ | $0.33 \pm 0.01$ |
| AZ2 | $143 \pm 9$ | $385 \pm 14$ | $0.37 \pm 0.03$ |
| Bosentan+AZ2 | $144 \pm 6$ | $377 \pm 10$ | $0.38 \pm 0.02$ |
| Phentolamine+AZ2 | $67 \pm 7$* | $412 \pm 11$ | $0.16 \pm 0.02$*** |

Results are expressed as Mean $\pm$ SEM (n=3-4/group). Comparisons between all treatment groups and Vehicle were made using ANOVA followed up by a Dunnett's multiple comparison test. *P<0.05, ***P<0.001 versus Vehicle.

**Table S4**

Body weights and baseline cardiovascular variables in anesthetized, ventilated dogs measured during the 15 min baseline period before infusion of vehicle or AZ2. Supporting information to Figures 8, 9 and S3. There were no significant differences between the 2 groups in any of the baseline parameters (Students t-test, P>0.05).

| | Vehicle | AZ2 |
|---|---|---|
| Body weight (kg) | 14.0 ± 1.0 | 14.6 ± 1.4 |
| No. per group (male/female) | 4 (2/2) | 4 (2/2) |
| MAP (mmHg) | 126 ± 5 | 102 ± 10 |
| HR (bpm) | 172 ± 7 | 167 ± 10 |
| CO (ml/min) | 2220 ± 271 | 2489 ± 254 |
| TPR ($Ns/m^5/10^6$) | 471 ± 51 | 336 ± 45 |
| CVP (mmHg) | 7.4 ± 0.7 | 7.0 ± 0.7 |
| RAF (ml/min) | 105 ± 10 | 110 ± 7 |
| RAR ($Ns/m^5/10^6$) | 9976 ± 1322 | 7557 ± 1193 |
| FAF (ml/min) | 125 ± 30 | 128 ± 14 |
| FAR ($Ns/m^5/10^6$) | 10087 ± 3031 | 6608 ± 972 |
| DCAF (ml/min) | 24.6 ± 3.7 | 16.6 ± 2.5 |
| DCAR ($Ns/m^5/10^6$) | 44856 ± 8891 | 51146 ± 6200 |

MAP, mean arterial pressure; HR, heart rate, CO, cardiac output; TPR, total peripheral resistance; CVP, central venous pressure; RAF, left renal artery flow; RAR, left renal artery resistance; FAF, left femoral artery flow, FAR, left femoral artery resistance; DCAF, left descending coronary artery flow; DCAR, left descending coronary artery resistance. Results are reported as Mean ± SEM.

**Table S5**

AZ2 was infused in dose response experiments to anaesthetized dogs. This table shows the linear relationship between AZ2 infusion rate and the AZ2 plasma concentration at the end of each 15 min infusion period, supporting information to Figures 8, 9 and S3.

| | Infusion Rate (nmol/kg/min) | Plasma Concentration (μM) |
|---|---|---|
| Baseline | 0.0 | LLOQ |
| Dose 1 | 5.5 | 0.054 ± 0.009 |
| Dose 2 | 16.5 | 0.157 ± 0.039 |
| Dose 3 | 55.0 | 0.596 ± 0.077 |
| Dose 4 | 165.0 | 1.683 ± 0.247 |
| Dose 5 | 550.0 | 5.130 ± 0.580 |
| Washout 1 | 0.0 | 1.074 ± 0.121 |
| Washout 2 | 0.0 | 0.855 ± 0.115 |

LLOQ, less than lower limit of quantification (0.03 μM). Results are expressed as Mean ± SEM, n=4/group.

**Table S6**

Absolute values of baseline cardiovascular variables in a study to investigate the effect of AZ2 on renal blood flow. Supporting information to Figure 10. Adult male Wistar rats were anesthetized and implanted with jugular and carotid catheters. Laparotomy was performed and a flow probe attached to the left renal artery, abdomen closed and animals were left for a 1h recovery. Mean arterial pressure (MAP), heart rate (HR), renal blood flow and vascular resistance data, represent values averaged over the 10 min baseline period immediately before intravenous infusion of vehicle or AZ2. The Bos+AZ2 group was pre-treated with the dual ET-A/B receptor antagonist, bosentan, 15 mg/kg i.v. just prior to the baseline period. There were no significant differences between the groups in any of the baseline parameters (1-way ANOVA, $P>0.05$). Results are expressed as Mean±SEM (Vehicle, n=6; AZ2, n=7; Bos+AZ2, n=4).

| | Vehicle | AZ2 | Bosentan+AZ2 |
|---|---|---|---|
| MAP (mmHg) | $119 \pm 9$ | $121 \pm 5$ | $118 \pm 11$ |
| HR (bpm) | $385 \pm 7$ | $383 \pm 8$ | $390 \pm 10$ |
| Left Renal Artery Blood Flow (ml/min) | $7.0 \pm 0.8$ | $7.3 \pm 0.9$ | $7.5 \pm 0.9$ |
| Renal Vascular Resistance ($Ns/m^5/10^9$) | $145 \pm 16$ | $148 \pm 23$ | $129 \pm 15$ |

MAP, mean arterial blood pressure; HR, heart rate.

**Supplementary Methods**

*Synthesis of AZ1.* 2-Chloro-4-ethoxy-*N*-[[6-[(1-methyl-4-piperidyl)sulfonyl]-1,3-benzothiazol-2-yl]carbamoyl]-5-pyrazol-1-yl-benzamide

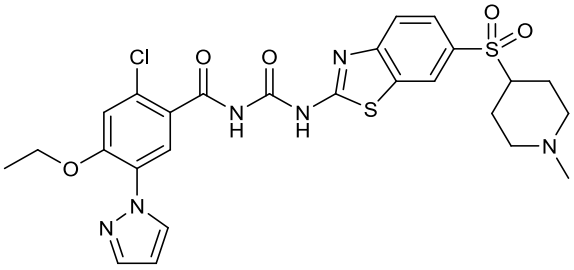

1) 2-Chloro-4-ethoxy-benzonitrile

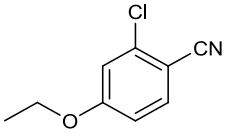

To a solution of 2-chloro-4-hydroxy-benzonitrile (10.00 g, 65.12 mmol) in DMA (*N,N*-dimethylacetamide) (100 mL) was added potassium carbonate (18.00 g, 130.24 mmol) followed by iodoethane (6.05 mL, 74.89 mmol) in portions. The cloudy reaction mixture was stirred at room temperature overnight. Ice/water was added to give a precipitate which was filtered off and washed with water. The solid was dissolved in acetonitrile and then evaporated to dryness (repeated 3 times) to give 2-chloro-4-ethoxy-benzonitrile as a colorless solid (98 %, 11.56 g). $^1$H NMR (300 MHz, $CDCl_3$) $\delta$ 1.45 (t, 3H), 4.09 (q, 2H), 6.85 (dd, 1H), 7.00 (d, 1H), 7.57 (d, 1H).

2) 2-Chloro-4-ethoxy-5-iodo-benzonitrile

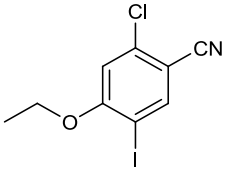

To a solution of 2-chloro-4-ethoxy-benzonitrile (10.00 g, 53.96 mmol) and trifluoromethanesulfonic acid (1.43 mL, 16.19 mmol) in acetonitrile (160 mL) was added NIS (*N*-iodosuccinimide) (13.33 g, 59.26 mmol) in portions over 15 min after which the reaction was stirred at room temperature overnight. A solution of sodium pyrosulfite (5.31 g) in water (50 mL) was added to the reaction mixture to give a thick precipitate which was diluted with water (110 mL). After being stirred for 30 min, the precipitate was filtered off and washed with water to give the expected product and an unwanted regioisomer in ca 9:1 ratio. Recrystallization from hot *i*-PrOH gave 2-chloro-4-ethoxy-5-iodo-benzonitrile (71 %, 11.74 g) as a single regioisomer. $^1$H NMR (300 MHz, $CDCl_3$) $\delta$ 1.54 (t, 3H), 4.16 (q, 2H), 6.86 (s, 1H), 8.01 (s, 1H).

3) 2-Chloro-4-ethoxy-5-pyrazol-1-yl-benzonitrile

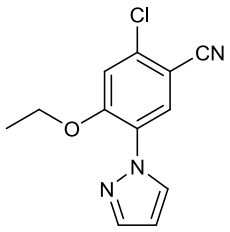


(*1R*,*2R*)-*N*1,*N*2-dimethylcyclohexane-1,2-diamine (0.694 g, 4.88 mmol) was added to 2-chloro-4-ethoxy-5-iodo-benzonitrile (5.00 g, 16.26 mmol), 1H-pyrazole (1.66 g, 24.39 mmol), potassium carbonate (4.49 g, 32.52 mmol), $Pd_2(dba)_3$ (1.68 g, 1.63 mmol) and copper(I) iodide (0.31 g, 1.63 mmol) in 1,4-dioxane (60 mL) at 25 °C under nitrogen. The resulting mixture was stirred under nitrogen at 95 °C for 45 h. The reaction mixture was diluted with EtOAc and filtered through celite. The filtrate was concentrated under reduced pressure and the crude product was purified by silica gel flash chromatography (gradient 0 to 20% EtOAc in petroleum ether) to give a yellow solid. The solid was triturated with methanol, filtered,

washed with methanol and dried under vacuum to afford 2-chloro-4-ethoxy-5-pyrazol-1-yl-benzonitrile (45 %, 1.80 g) as a colourless solid. MS m/z (ES+), $[M+H]^+$ = 248; $^1$H NMR (300 MHz, DMSO-$d_6$) $\delta$ 1.37 (t, 3H), 4.30 (q, 2H), 6.54 (t, 1H), 7.64 (s, 1H), 7.77 (d, 1H), 8.17 (s, 1H), 8.27 (t, 1H).

4) 2-Chloro-4-ethoxy-5-pyrazol-1-yl-benzamide

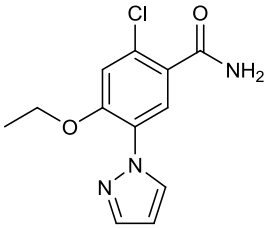


To a mixture of 2-chloro-4-ethoxy-5-pyrazol-1-yl-benzonitrile (16.50 g, 66.62 mmol) and potassium carbonate (4.60 g, 33.31 mmol) in DMSO (200 mL) was added hydrogen peroxide (20 ml, 652.66 mmol) at 10 °C. The resulting mixture was stirred at 25 °C for 3 h and then quenched with water (500 mL). The precipitate was collected by filtration, washed with water (300 mL) and dried under vacuum to afford 2-chloro-4-ethoxy-5-pyrazol-1-yl-benzamide (97 %, 17.20 g) as a colorless solid, which was used directly in the next step without further purification. MS m/z (ES+), $[M+H]^+$ = 266; $^1$H NMR (300 MHz, DMSO-$d_6$) $\delta$ 1.36 (t, 3H), 4.22 (q, 2H), 6.52 (t, 1H), 7.35 (s, 1H), 7.57 (d, 1H), 7.74-7.77 (m, 2H), 7.87 (s, 1H), 8.27 (d, 1H).

5) Phenyl *N*-(2-chloro-4-ethoxy-5-pyrazol-1-yl-benzoyl)carbamate

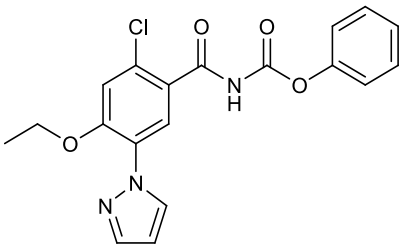

A suspension of 2-chloro-4-ethoxy-5-pyrazol-1-yl-benzamide (17.20 g, 64.74 mmol) and diphenyl carbonate (20.80 g, 97.10 mmol) in anhydrous THF (500 mL) was cooled to 0 °C. Sodium hydride (2.02 g, 84.16 mmol) was added in portions over a period of 30 min. The resulting mixture was allowed to attain room temperature and stirred for 3 h. The reaction mixture was quenched with acetic acid (50 mL). The reaction mixture was diluted with EtOAc and washed with water (5 x 300 mL). The organic phase was dried, filtered and evaporated. The residue was purified by silica gel flash chromatography (gradient 0 to 50% EtOAc in DCM) to give phenyl *N*-(2-chloro-4-ethoxy-5-pyrazol-1-yl-benzoyl)carbamate (88 %, 22.00 g) as a colourless solid. MS m/z (ES+), $[M+H]^+$ = 386; $^1$H NMR (300MHz, DMSO-$d_6$) $\delta$ 1.37 (t, 3H), 4.25 (q, 2H), 6.53 (t, 1H), 7.20-7.31 (m, 3H), 7.41-7.46 (m, 3H), 7.76 (s, 1H), 7.90 (s, 1H), 8.29 (d, 1H), 11.74 (s, 1H).

6) 2-Chloro-4-ethoxy-*N*-[[6-[(1-methyl-4-piperidyl)sulfonyl]-1,3-benzothiazol-2-yl]carbamoyl]-5-pyrazol-1-yl-benzamide

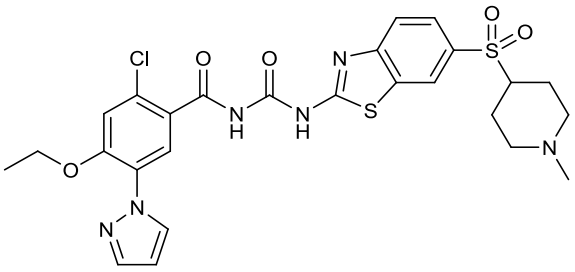


A suspension of 6-[(1-methyl-4-piperidyl)sulfonyl]-1,3-benzothiazol-2-amine (McCoull W *et al.,* J Med Chem 2014; 57(14): 6128-6140) (10.50 g, 33.72 mmol) and phenyl *N*-(2-chloro-4-ethoxy-5-pyrazol-1-yl-benzoyl)carbamate (12.00 g, 31.10 mmol) in toluene (400 mL) was heated at 100 °C for 14 h. The solvent was removed under reduced pressure. The crude product was purified by silica gel flash chromatography (gradient 0 to 5% MeOH in DCM) to give 2-chloro-4-ethoxy-*N*-[[6-[(1-methyl-4-piperidyl)sulfonyl]-1,3-benzothiazol-2-

yl]carbamoyl]-5-pyrazol-1-yl-benzamide (79 %, 14.90 g) as a colourless solid. MS m/z (ES+), $[M+H]^+$ = 603; $^1$H NMR (300 MHz, DMSO-$d_6$) $\delta$ 1.38 (t, 3H), 1.51-1.62 (m, 2H), 1.83-1.99 (m, 4H), 2.18 (s, 3H), 2.88 (d, 2H), 3.19-3.28 (m, 1H), 4.27 (q, 2H), 6.54 (t, 1H), 7.44 (s, 1H), 7.76 (d, 1H), 7.81(dd, 1H), 7.90 (d, 1H), 7.98 (s, 1H), 8.30 (d, 1H), 8.53 (d, 1H), 11.66 (brs, 2H) . $^{13}$C NMR (500MHz, DMSO-$d_6$) $\delta$ 14.2, 24.6, 45.0, 53.2, 59.4, 65.4, 107.1, 115.1, 120.2, 123.6, 124.9, 126.2, 126.5, 127.5, 129.4, 130.5, 131.7, 132.5, 140.4, 151.5, 151.9, 152.5, 163.8, 167.2; ESI-HRMS calculated for $C_{26}H_{28}ClN_6O_5S_2$ $[M+H]^+$ 603.1251; found, 603.1260. HPLC purity >98 %.

*Synthesis of AZ2.* 2-Chloro-4-ethoxy-*N*-[[6-[(4-methylpiperazin-1-yl)methyl]-1,3-benzothiazol-2-yl]carbamoyl]-5-morpholino-benzamide

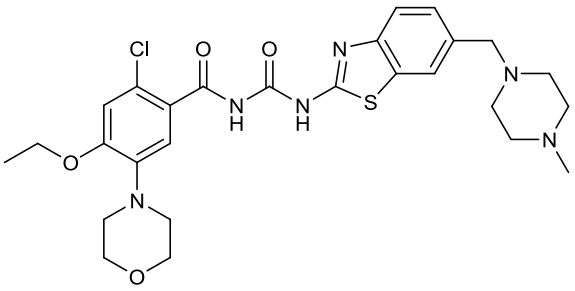


1) 2-Chloro-4-ethoxy-5-morpholino-benzonitrile

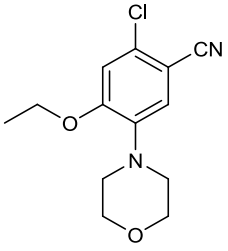


A 1L three neck round bottom flask was charged with 2-chloro-4-ethoxy-5-iodo-benzonitrile (20.00 g, 65.04 mmol), cesium carbonate (29.70 g, 91.05 mmol), 2,2'-

bis(diphenylphosphino)-1,1'-binaphthyl (rac-BINAP) (1.42 g, 2.28 mmol) and diacetoxypalladium (0.365 g, 1.63 mmol). The flask was evacuated and filled with nitrogen (repeated 3 times). Nitrogen purged toluene (200 mL) was added and the reaction mixture was purged with nitrogen for 10 min and then heated to 70-75 °C. Nitrogen purged morpholine (17 mL, 195.11 mmol) was added dropwise and the mixture was heated at 105 °C for 20 h. The reaction mixture was allowed to attain room temperature and then diluted with water (150 mL), 2-Me-THF (100 mL) and acetonitrile (50 mL). The phases were separated and the organic phase was washed with water, dried and concentrated under vacuum. The crude solid was triturated with MeOH, filtered, washed with MeOH and *i*-PrOH and dried to give 2-chloro-4-ethoxy-5-morpholino-benzonitrile (66 %, 11.50 g) as a light yellow solid. MS m/z (ES+), $[M+H]^+$ = 267; $^1$H NMR (400 MHz, $CDCl_3$) $\delta$ 1.49 (t, 3H), 3.05 (m, 4H), 3.86 (m, 4H), 4.11 (q, 2H), 6.89 (s, 1H), 7.06 (s, 1H).

2) 2-Chloro-4-ethoxy-5-morpholino-benzamide

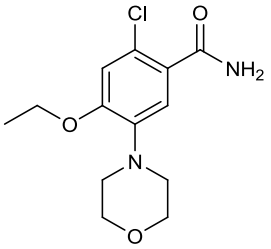


To a mixture of 2-chloro-4-ethoxy-5-morpholino-benzonitrile (5.00 g, 18.75 mmol) and hydrogen peroxide (30 %, 116 mL) in ethanol (50 mL) was added pellets of sodium hydroxide (4.69 g, 117.25 mmol) in portions during 6 h to minimize foaming. The reaction mixture was then stirred at room temperature for 48 h. Water was added to the reaction mixture and the precipitate was filtered off, washed with water and dried to give a solid. The filtrate was extracted with 2-Me-THF, the organic phase was dried, filtered and evaporated to give a

solid. The combined solids were slurried in acetonitrile, filtered and dried to give 2-chloro-4-ethoxy-5-morpholino-benzamide (100 %, 5.34 g) as a light yellow solid. MS m/z (ES+), $[M+H]^+$ = 285; $^1$H NMR (400 MHz, $CDCl_3$) $\delta$ 1.48 (t, 3H), 3.10 (m, 4H), 3.87 (m, 4H), 4.11 (q, 2H), 5.93 (bs, 1H), 6.67 (bs, 1H), 6.83 (s, 1H), 7.51 (s, 1H).

3) Phenyl *N*-(2-chloro-4-ethoxy-5-morpholino-benzoyl)carbamate

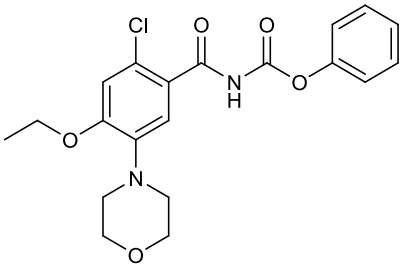


A suspension of 2-chloro-4-ethoxy-5-morpholino-benzamide (2.00 g, 7.02 mmol) and diphenyl carbonate (1.73 g, 8.08 mmol) in anhydrous THF (25 mL) was cooled to 0 °C. Sodium hydride (0.365 g, 9.13 mmol) was added in portions over 5 min. The reaction mixture was allowed to attain room temperature and stirred for 40 min. The reaction was quenched by addition of acetic acid (1.20 mL), diluted with DCM (100 mL), washed with water (50 mL), dried, filtered and evaporated. The residue was triturated with heptane/ethyl acetate (9:1), filtered off and dried to give phenyl *N*-(2-chloro-4-ethoxy-5-morpholino-benzoyl)carbamate (81 %, 2.30 g) as a colorless solid. MS m/z (ES+), $[M+H]^+$ = 405; $^1$H NMR (400 MHz, $CDCl_3$) $\delta$ 1.50 (t, 3H), 3.10 (m, 4H), 3.88 (m, 4H), 4.12 (q, 2H), 6.86 (s, 1H), 7.18-7.22 (m, 2H), 7.34 (s, 1H), 7.37-7.43 (m, 3H), 8.63 (bs, 1H).

4) 2-Chloro-4-ethoxy-*N*-[[6-[(4-methylpiperazin-1-yl)methyl]-1,3-benzothiazol-2-yl]carbamoyl]-5-morpholino-benzamide

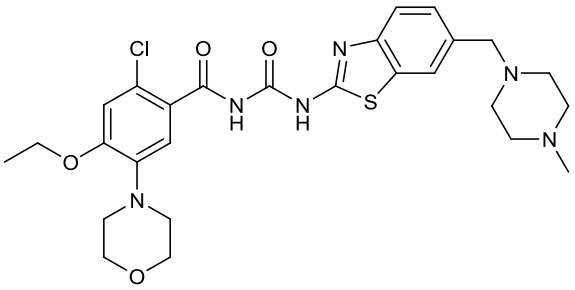


A suspension of phenyl *N*-(2-chloro-4-ethoxy-5-morpholino-benzoyl)carbamate (3.00 g, 7.41 mmol) and 6-[(4-methylpiperazin-1-yl)methyl]-1,3-benzothiazol-2-amine (1.94 g, 7.41 mmol) in toluene (100 mL) was heated at 100 °C for 13 h. The solvent was removed under reduced pressure and the crude product was purified by silica gel flash chromatography (gradient 0 to 10% MeOH in DCM) to give 2-chloro-4-ethoxy-*N*-[[6-[(4-methylpiperazin-1-yl)methyl]-1,3-benzothiazol-2-yl]carbamoyl]-5-morpholino-benzamide (1.50 g, 35.3 %) as a colourless solid. MS m/z (ES+), $[M+H]^+$ = 573; $^1$H NMR (DMSO-$d_6$, 300MHz) $\delta$ 1.37 (t, 3H), 2.07-2.50 (m, 11H), 3.03 (b, 4H), 3.55 (s, 2H), 3.74 (b, 4H), 4.10-4.17 (m, 2H), 7.10 (s, 1H), 7.16 (s, 1H), 7.36 (d, 1H), 7.69 (d, 1H), 7.89 (s, 1H), 11.56-11.81 (b, 2H). $^{13}$C NMR (500 MHz, DMSO-$d_6$) $\delta$ 14.4, 45.6, 50.2, 52.5, 54.6, 61.9, 64.2, 66.1, 113.9, 118.9, 120.1, 121.6, 124.4, 125.1, 127.3, 131.8, 134.0, 139.4, 147.7, 151.0, 153.5, 157.5, 168.4; ESI-HRMS calculated for $C_{27}H_{34}ClN_6O_4S$ $[M+H]^+$ 573.2051; found, 573.2089. HPLC purity >98 %.

*In vitro characterization of GPR81 activity and inhibition of lipolysis in rat and human adipocytes*.

*cAMP assay for identification of GPR81 and GPR109A agonism*. T-REx™-CHO cells (Life Technologies) were transfected with human GPR81 or GPR109A receptors and stable clones were cryopreserved for later use. For each experiment cells were thawed in a 37°C water bath, centrifuged (180g) and then re-suspended in assay buffer (HBSS/Hepes buffer, pH 7.4, containing 0.1% BSA). Assays were performed at room temperature according to the

protocol described in the cAMP assay kit (PerkinElmer LANCE® cAMP Detection Kit) with minor modifications. Two µl cell suspension (500 cells per well) was added to 1536-well microplates pre-dispensed with 40 nl screening compounds dissolved in DMSO (half-log dilution series to constitute 10 point concentration response curves in quadruplicate) and incubated for 30 min followed by addition of 2 µl forskolin solution (containing anti-cAMP antibody labelled with Alexa Fluor® 647) to stimulate cAMP production. After 20 min the incubation was terminated by addition of 2 µl detection mix (containing Europium-labelled cAMP) and the fluorescent signal (665/615nm emission ratio; excitation wavelength: 340 nm) was measured using a PHERAstar (BMG Labtech) microplate reader. TR-FRET values were converted to nM cAMP using a cAMP standard curve. The maximal effect (efficacy) was defined using a selective AstraZeneca R&D in-house developed agonist for the GPR81 assay (compound with same efficacy as lactate) or nicotinic acid for the GPR109A assay. The Z'-Factor was typically between 0.5 to 0.6. $EC_{50}$ and efficacy values were calculated by fitting concentration response curves to a four-parameter logistic non-linear regression model using Genedata Screener® software.

*Isolation of primary mature rat adipocytes.* Epididymal adipose tissue was collected from isoflurane anesthetized, overnight fasted male Sprague Dawley rats (Charles River, Netherlands) weighing 250-300 g. Directly after dissection, the fat pads were placed into a 50 ml tube containing PBS (Gibco) and PEST (Life Technologies, Grand Island, NY). Within 10 min of tissue collection isolation of the adipocytes was initiated. The fat pads were cut into small pieces and incubated for 30-45 min in Krebs Ringer HEPES (KRH) buffer supplemented with 2 mM glucose (Sigma, St. Louis, MO), 0.2 µM Adenosine (Sigma) and 0.4 mg/ml Type 2 collagenase (Worthington, Lakewood, NJ). After collagenase treatment, the suspension was poured through a 250 µm mesh filter. The resulting filtrate was briefly centrifuged 1 min to

separate the mature adipocytes from other cell debris. Floating mature adipocytes were washed twice in KRH buffer and counted.

*Isolation of primary mature human adipocytes.* Mature human adipocytes were isolated from human subcutaneous white adipose tissue collected at Sahlgrenska University Hospital (Gothenburg) from patients undergoing cosmetic surgery. The same isolation procedure was used for the human adipocytes as the rodent adipocytes with the exception of that the purified adipocytes were incubated overnight in 1 vol. KRH, 2 vol. DMEM and 0.5 µM Adenosine, prior use.

*In vitro lipolysis assay.* Test compounds, 1 µL dissolved in DMSO, were pipetted into flat bottom 96 well Microtiter plates. Before start of the assay the compounds were diluted with 9 µL KRH buffer. Eighty µL (3-4*$10^5$ cells/ml) of mature adipocytes were dispensed into each well using an 8-channel pipette with wide orifice tips. Cells were incubated for 10 min at 37°C in an iEMS incubator/shaker (Thermo Scientific, Vantaa, Finland) prior the addition of 10 µL KRH buffer containing 0.1 U/ml Adenosine deaminase (ADA), (Roche, Mannheim Germany) and the calculated $EC_{80}$ value of forskolin (Calbiochem, Billerica, MA) to activate lipolysis. ADA degrades adenosine and Forskolin activates adenylyl cyclase and addition of both leads to maximal intracellular cAMP levels and hydrolysis of triglycerides into fatty acids and glycerol. Plates were incubated in the iEMS incubator/shaker for 2 h. After incubation, 20 µL of the supernatant was carefully removed using a Biomek Robot system (Beckman Coulter, Brea, CA), avoiding any cells, into a new 96-well plate for analysis of glycerol levels. 200 µL of glycerol reagent (Sigma) was added to each well and then the plate was incubated at 37°C for 10 min before reading the optical density at 540 nm (Spectramax Reader, Molecular Devices, Sunnyvale, CA). The release of glycerol was calculated as %

inhibition in relation to maximum inhibition (based on effects of an in-house hormone sensitive lipase inhibitor) and minimum inhibition (forskolin).

*ob/ob study.* Eight week old male ob/ob mice (B6.V-Lep^ob/OlaHsd, Harlan Laboratories) were divided into vehicle (4 % DMA) or AZ1 (20 µmol/kg/day q.d.) groups based on average body weight for each cage of 4 mice two days before the dosing was initiated (n=8/group). Mice were dosed (5 ml/kg) in the afternoon at 3 pm each day for 2 weeks. On the final day, the mice were dosed at 7 am and then fasted for 3 h before blood sampling. Blood was collected from isoflurane anesthetized mice into EDTA tubes which were immediately placed on ice before centrifugation. Plasma was stored at -20°C until analysis.